KFUPM
Journal of Undergraduate Research International

Diamond Open Access 113

Article Material Science and Engineering

# Single-Step Synthesis of Sheet-Like Graphitic Carbon Nitride from Thiourea for Photodegradation of Methylene Blue

Hashim Zaki Alsadah and Muhammad Ihsan-Ul-Haq*

Cite https://doi.org/10.64589/juri/231541

**Submitted:** April 25, 2026 **Revised:** May 09, 2026 **Accepted:** May 11, 2026

**ABSTRACT**

The development of effective photocatalytic materials for organic-pollutant degradation remains a critical undertaking in the field of environmental materials. Graphitic carbon nitride (g-$C_3N_4$) is a widely studied metal-free photocatalyst for environmental remediation because of its chemical stability, low cost, and semiconductor response under light irradiation. However, melamine-derived g-$C_3N_4$ must be subjected to additional processing, such as exfoliation, freeze–drying, or morphology-control treatments, to overcome its low surface area and rapid charge-carrier recombination. In this work, sheet-like g-$C_3N_4$ structures are synthesized from thiourea through a single-step thermal polycondensation route, followed only by manual crushing in an agate mortar. Photocatalytic testing using an aqueous methylene blue (MB) model solution under irradiation from a 60 W light-emitting diode (395 nm) reveals ~90% dye degradation within 75 min, corresponding to an apparent pseudo-first-order rate constant of approximately ~3.28 $\times 10^{-2}$ $min^{-1}$. Although the proposed catalyst does not outperform existing melamine-based g-$C_3N_4$ systems reported for MB degradation, it offers a strong balance between production simplicity and performance because the sheet-like morphology is achieved without post-synthesis exfoliation, freeze–drying, or composite formation. Overall, this study establishes precursor engineering as a practical and facile strategy for improving the performance of g-$C_3N_4$ photocatalysts for dye remediation.

**Keywords:** photocatalysis, graphitic carbon nitride, thiourea, methylene blue, wastewater remediation

## 1. INTRODUCTION

Since its introduction in 2009[1], polymeric graphitic carbon nitride (g-$C_3N_4$) has emerged as a key metal-free photocatalyst for solar and environmental applications[2–5] owing to its favorable composition involving earth-abundant elements, chemical robustness, and layered conjugated framework[6]. Notwithstanding these benefits, bulk g-$C_3N_4$ exhibits a limited surface area and rapid electron–hole recombination, which suppress photocatalytic efficiency. To address these limitations, extensive research efforts have been devoted to structural tuning and nanostructuring[7–10]. Melamine remains one of the most commonly used precursors for g-$C_3N_4$ synthesis[11,12]. However, melamine-derived materials must typically be subjected to additional treatments, such as thermal exfoliation[13] and freeze–drying-based nanostructuring[14], to improve their photocatalytic efficacy.

Precursor selection has been established as a powerful strategy for tuning the microstructure and photocatalytic behavior of g-$C_3N_4$. For instance, in a direct comparison of melamine- and urea-derived g-$C_3N_4$, the urea-derived material displayed smaller crystallites, a slightly narrower band gap, a larger surface area, and superior dye-degradation performance than its melamine-derived counterpart[15]. Additionally, a recent precursor-dependent study comparing exfoliated g-$C_3N_4$ produced from melamine and thiourea reported more efficient degradation of crystal violet (CV) and malachite green (MG) dyes for the thiourea-derived g-$C_3N_4$, attributable to its narrower band gap, larger surface area, and greater pore volume[16]. These studies indicate that precursor chemistry considerably influences porosity, accessible surface area, light-absorption capacity, and charge transport even before composite formation or heterojunction engineering is initiated[17–19].

The use of methylene blue (MB) in industries such as textile production has led to several environmental and health concerns because of its toxicity, carcinogenic and mutagenic behavior, and environmental impacts[20–22]. Considering these aspects, this study is aimed at establishing a facile strategy for synthesizing g-$C_3N_4$ for MB degradation. Leveraging precursor engineering, g-$C_3N_4$ is synthesized using thiourea via single-step thermal polycondensation. Unlike conventional melamine-derived systems that require additional treatments to enhance performance, the proposed precursor selection strategy alone induces favorable morphological characteristics and affords competitive photocatalytic activity. The derived g-$C_3N_4$ achieves ~90% MB degradation within 75 min. Overall, this work offers a low-complexity alternative to multi-step material engineering approaches, such as ball milling, hydrothermal composite assembly, or post-exfoliation to enhance surface area.


Published under an exclusive license by KFUPM

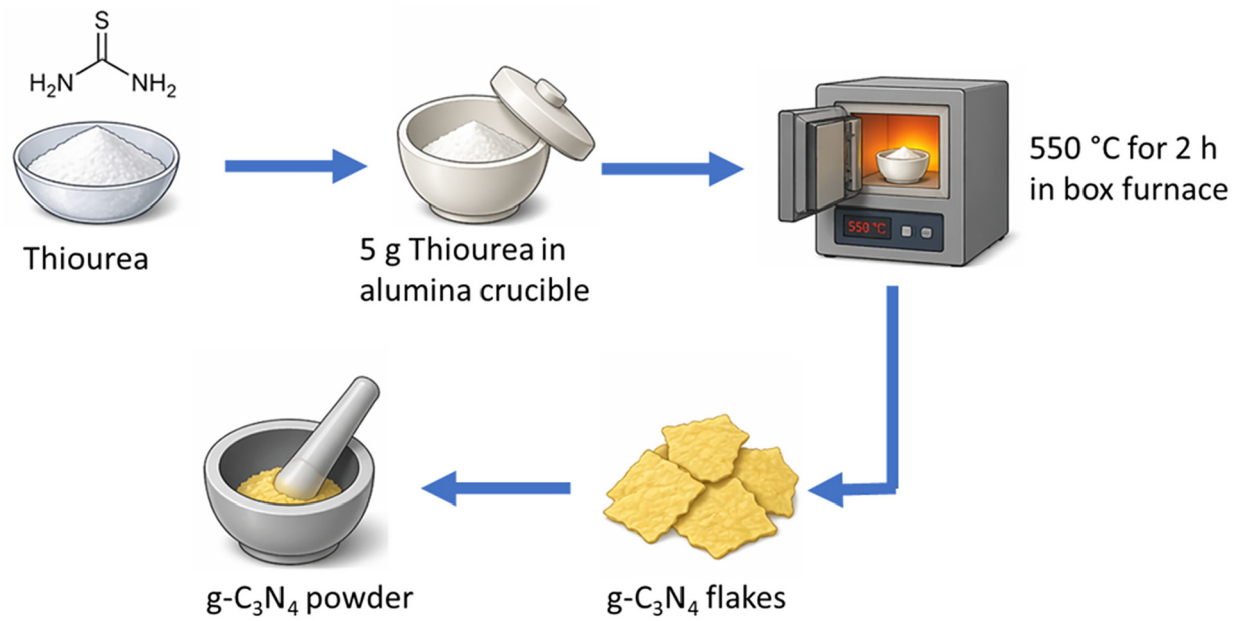


**Figure 1.** Schematic of the synthesis of g-$C_3N_4$ powder

## 2. EXPERIMENTAL PROCEDURE

**2.1. Materials and Synthesis.** Thiourea (>99% purity, Sigma-Aldrich, USA) was used as the precursor for g-$C_3N_4$ synthesis. MB (≥95% purity, HPLC grade, Sigma-Aldrich) was used as the model dye pollutant without further purification. Deionized (DI) water was used to prepare the model 0.5 mM dye solution.

As illustrated in Figure 1, 5 g of thiourea was transferred to an alumina crucible with a lid. The covered crucible was placed in a box furnace and heated to 550 °C at a rate of 10 °C per minute. The furnace was maintained at 550 °C for 120 min and then allowed to cool naturally to room temperature (24 °C), yielding g-$C_3N_4$ flakes. The resulting g-$C_3N_4$ was manually crushed using an agate mortar and pestle to obtain a powder suitable for characterization and photocatalytic testing.

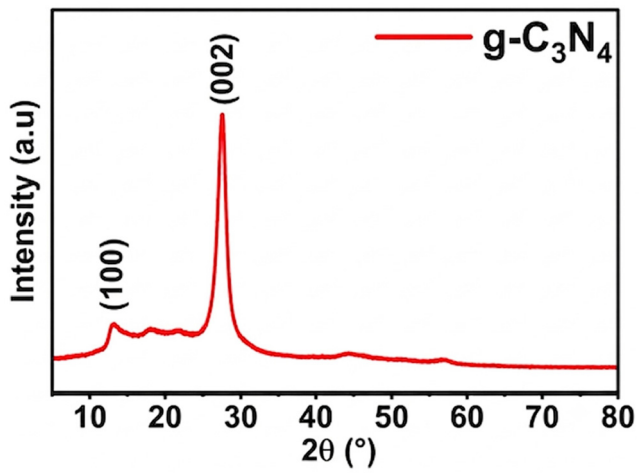


**Figure 2.** XRD pattern of g-$C_3N_4$ powder showing characteristic peaks at the 002 and 100 planes

**2.2. Materials Characterization.** X-ray diffraction (XRD) patterns were recorded using Cu K$\alpha$ radiation ($\lambda = 1.5406$ Å) over a $2\theta$ range of 5°–80°with a step size of 0.1°. The morphology and nanostructure of the synthesized g-$C_3N_4$ were examined by scanning electron microscopy (SEM, JEOL 5800LV) coupled with energy-dispersive spectroscopy (EDS) and transmission electron microscopy (TEM, JEM-2100F).

An ultraviolet–visible (UV–vis) spectrophotometer (Cary 60, Agilent Technologies) was used to evaluate the photocatalytic activity of g-$C_3N_4$ in an aqueous MB solution. Specifically, 75 mg of g-$C_3N_4$ was dispersed in 50 mL of the MB dye solution and stirred at 750 rpm for 30 min in the dark to establish adsorption–desorption equilibrium. The solution was then divided into two beakers with identical sizes. One beaker was wrapped in aluminum foil and placed in a dark closed space to ensure that any observed degradation corresponded to self-decomposition of the dye under dark conditions. The other beaker was irradiated using a 60 W UV light-emitting diode (LED) floodlight. To assess the photocatalytic performance of the as-synthesized g-$C_3N_4$, aliquots were collected at 15-min intervals separately from the beaker placed under dark conditions and the beaker subjected to UV irradiation. These aliquots were transferred to a quartz cuvette with a path length of 1 cm to acquire UV–vis spectra. The degradation kinetics were analyzed using a pseudo-first-order model (Equation 1), where $C_0$ is the initial concentration, $C_t$ is the concentration at irradiation time $t$, and $k$ is the apparent rate constant.

$$\ln\left(\frac{C_0}{C_t}\right) = kt \tag{1}$$

## 3. RESULTS AND DISCUSSION

**3.1. Structural and Morphological Analyses.** The XRD pattern (Figure 2) confirms the formation of g-$C_3N_4$. The

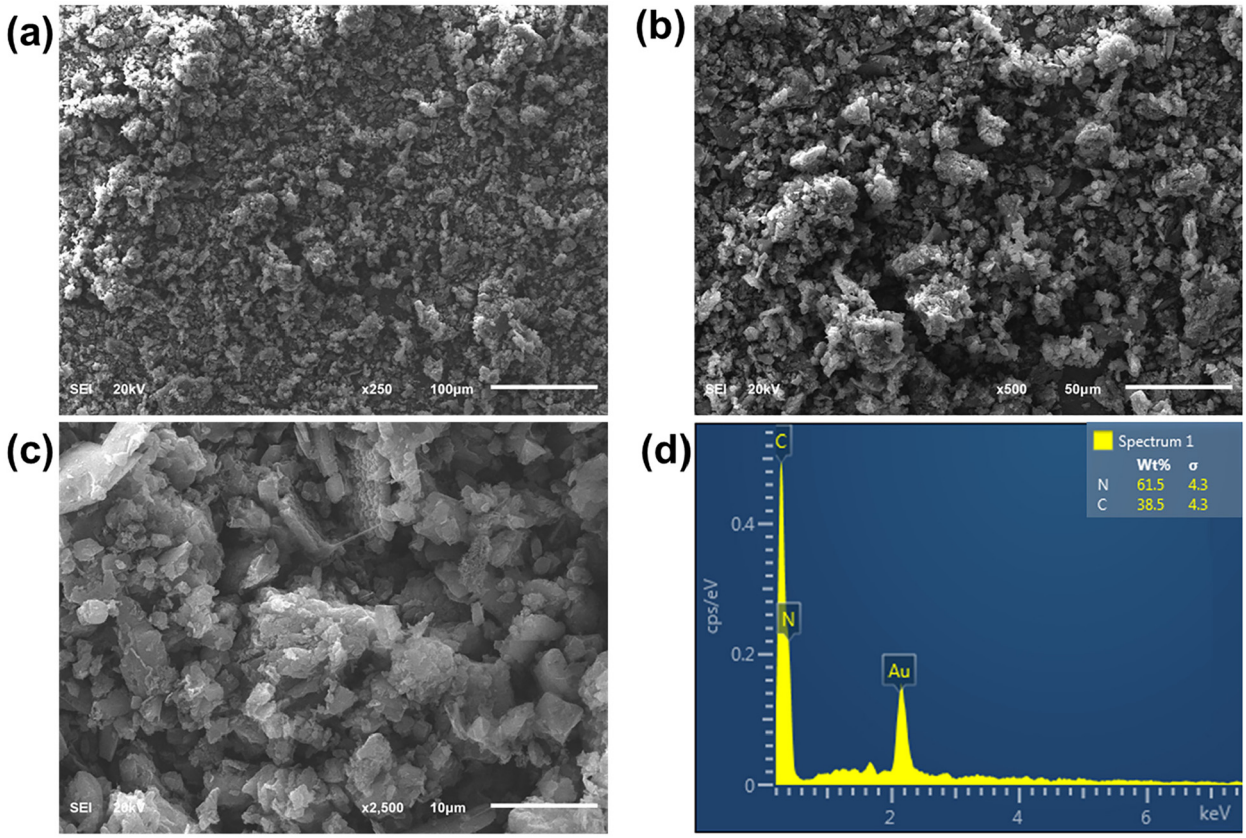


**Figure 3.** SEM micrographs at (a) 250X, (b) 500X, and (c) 2500X magnifications, and (d) EDS spectrum of g-$C_3N_4$ powder

observed pattern is consistent with the standard g-$C_3N_4$ fingerprint reported in the literature and matches well with JCPDS card No. 87-1526. The weak reflection near 13.1°is associated with in-plane structural ordering, whereas the strong peak near 27.3°corresponds to interlayer stacking of the conjugated aromatic layers[16]. This agreement supports successful formation of a layered g-$C_3N_4$ framework in the thiourea-derived sample.

SEM micrographs (Figure 3) show the g-$C_3N_4$ particles exhibit a nonuniform size and irregular morphology, indicating that the derived g-$C_3N_4$ is not a monodisperse powder but instead consists of agglomerated fragments formed during thermal polycondensation and manual crushing. The EDS spectrum indicates the presence of carbon (~38.5 wt.%) and nitrogen (~61.5 wt.%) in g-$C_3N_4$. The detected gold signal is attributable to the thin gold coating applied during SEM sample preparation. To obtain more detailed insights into the nanostructure, TEM analysis was performed. As shown in Figure 4, the g-$C_3N_4$ sample displays a loosely stacked, sheet-like morphology with void-like features. This morphology is favorable for photocatalysis; specifically, loosely stacked thin-sheet assemblies with apparent void features can expose a larger amount of interfacial surface to the dye solution and reduce diffusion limitations compared with dense bulk agglomerates. The loosely stacked sheet texture is also consistent with reports indicating that precursor selection strongly affects the final g-$C_3N_4$ microstructure. In particular, thiourea-derived g-$C_3N_4$ has been shown to exhibit a larger surface area and more favorable photocatalytic characteristics than melamine-derived counterparts, supporting the

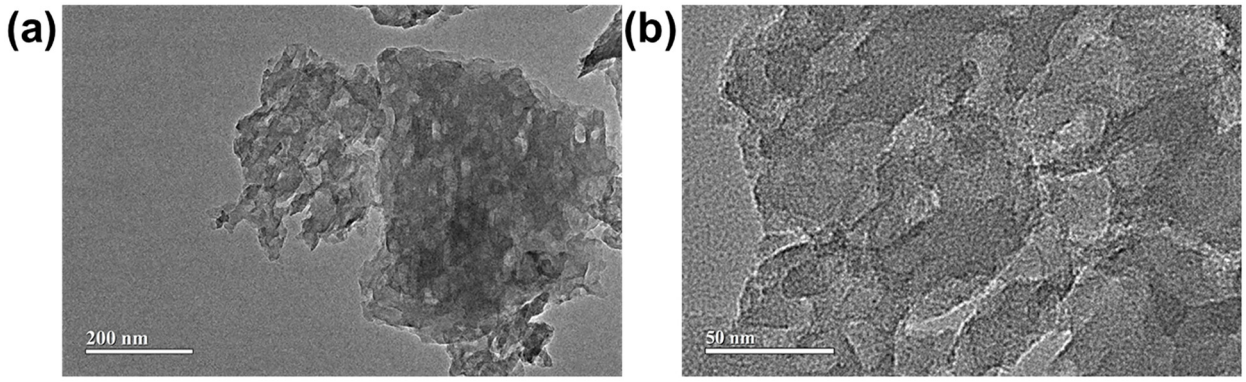


**Figure 4.** TEM micrographs of g-$C_3N_4$ powder at different magnifications, revealing a loosely stacked sheet-like structure

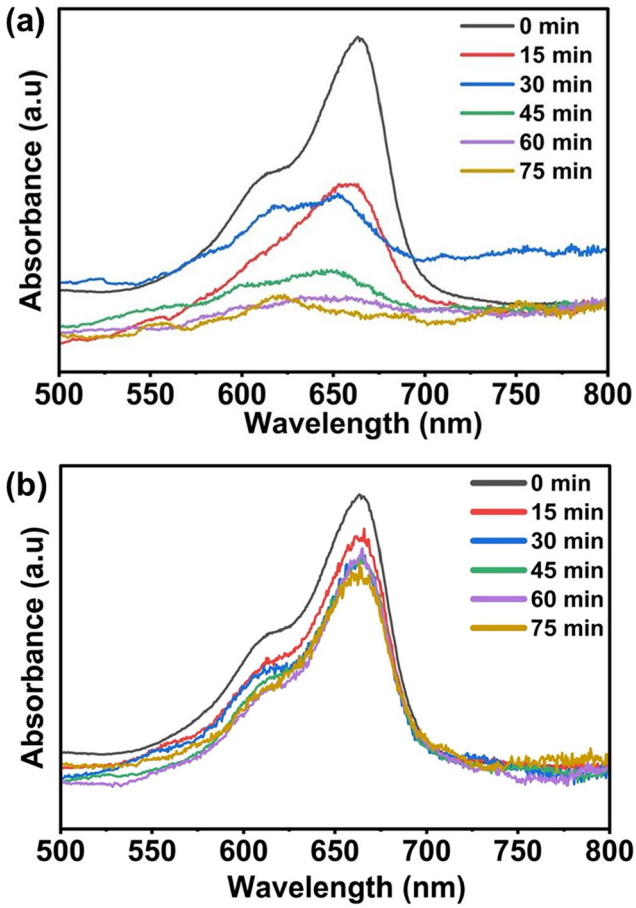


**Figure 5.** UV–vis spectra showing time-resolved photodegradation performance of MB using g-$C_3N_4$ photocatalysts under (a) UV irradiation and (b) dark conditions

interpretation that the porous morphology observed in this study is attributable to the use of thiourea [16].

**3.2. Photocatalytic Degradation of MB.** As shown in Figure 5a, the MB absorption band near 664 nm decreases during the irradiation period, corresponding to a ~90.86% decay in the MB concentration after 75 min. In contrast, the aliquots collected from the solution in the beaker kept under dark conditions show minimal decay in MB concentration (Figure 5b), indicating that the measured decline under irradiation is not dominated by initial mixing artifacts. The photocatalytic degradation kinetics were analyzed using a pseudo-first-order model by plotting $\ln(C_0/C_t)$ as a function of time (Figure 6). Linear fitting yielded an apparent rate constant ($k$) of approximately 3.28 $\times 10^{-2}$ $min^{-1}$ with a correlation coefficient ($R^2$) of approximately 0.96, confirming that the degradation follows pseudo-first-order kinetics. The measured constant indicates substantial photocatalytic activity for a metal-free catalyst prepared in a single step without any secondary exfoliation or composite assembly.

The obtained values are comparable to those reported for melamine-based g-$C_3N_4$ (Table 1), especially when synthesis simplicity is considered. For example, Molaei and Rahimi-Moghadam prepared porous g-$C_3N_4$ nanosheets via thermal polymerization of melamine in air and reported nearly 99% MB degradation in 60 min, with a rate constant of 6.49 $\times 10^{-2}$ $min^{-1}$ for the optimized sample synthesized at 700 °C [23]. Ganesan et al. synthesized bulk melamine-derived g-$C_3N_4$ and subjected it to thermal exfoliation. The material achieved 92% ±0.18% MB degradation within 60 min under UV irradiation, with the Brunauer–Emmett–Teller surface area increased from 5.03 to 48.20 $m^2$ $g^{-1}$ [13]. Surender and Balakumar prepared a freeze–dried melamine-derived nanostructured g-$C_3N_4$, which achieved 98.8% MB degradation in 40 min under visible light [14]. Attri et al. showed that exfoliated g-$C_3N_4$ nanosheets achieved 98.4% MB degradation within 60 min under visible light and were five times more efficient than the melamine-derived and mixed-precursor analogues [15]. Although that study focused on urea-, melamine-, and mixed-precursor systems rather than those derived from pure thiourea, it demonstrates that the precursor chemistry exerts a first-order influence on photocatalytic performance, even before the introduction of metals or composite development.

Compared with the existing frameworks, the thiourea-derived g-$C_3N_4$ obtained herein exhibits slightly slower absolute kinetics, achieving 90% degradation in 75 min with $k \approx 3.28 \times 10^{-2}$ $min^{-1}$. However, the proposed strategy offers notable advantages in synthetic simplicity. The material displays substantial activity without thermal exfoliation, freeze–drying, salt-assisted blowing, or heterojunction/composite fabrication. Thus, the main contribution of this study is not the realization of superior activity relative to melamine-derived system but rather the demonstration that competitive MB degradation activity can be achieved using precursor selection alone.

Under 395 nm irradiation, g-$C_3N_4$ generates photogenerated electrons and holes that react with dissolved oxygen and water-related species to form reactive oxidizing intermediates. In optimized melamine-derived g-$C_3N_4$ systems for dye degradation, superoxide radicals and holes have been identified as the dominant reactive species, with hydroxyl radicals playing a secondary role [13,23]. By analogy, the loosely stacked sheet-like morphology of the present thiourea-derived g-$C_3N_4$ likely facilitates oxygen access, interfacial charge transfer, and pollutant–catalyst contact.

Future work can be aimed at comparing the prepared material with a melamine-derived control synthesized under the same conditions and exploring its degradation mechanism.

## 4. CONCLUSIONS

Loosely stacked g-$C_3N_4$ sheets were successfully prepared from thiourea via single-step thermal polycondensation. XRD confirmed the formation of a layered g-$C_3N_4$ structure, while SEM and TEM analyses revealed the presence of irregular particles constituting several stacked sheets. The material achieved 90.86% degradation of MB within 75 min under 395 nm UV-LED irradiation, corresponding to an apparent pseudo-first-order rate constant of approximately 3.28 $\times 10^{-2}$ $min^{-1}$. Although this activity is not superior to that of optimized melamine-derived g-$C_3N_4$ systems reported for MB degradation, it is achieved without secondary exfoliation, freeze–drying, high-temperature processing (~700 °C), or composite formation. Overall, this work establishes precursor engineering, particularly the use of thiourea instead of melamine, as an effective low-complexity route to sheet-like and photoactive g-$C_3N_4$ for dye removal. Future work can be aimed at direct comparisons with

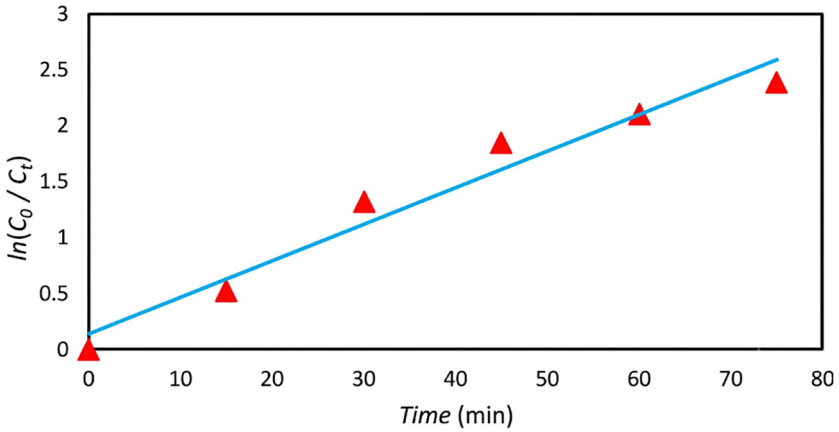


**Figure 6.** Photocatalytic degradation rate of MB as a function of time

**Table 1.** *Comparison of photocatalytic degradation of MB using g-$C_3N_4$ prepared via different precursors and preparation routes*

| Publication | Precursor | Preparation Method | Degradation (%) | Time (min) |
|---|---|---|---|---|
| **This study** | Thiourea | Thermal Polycondensation | 90.86 | 75 |
| **Molaei and Rahimi-Moghadam**[23] | Melamine | Thermal Polymerization | 99 | 60 |
| **Ganesan et al.**[13] | Melamine | Thermal Exfoliation | 92 ±0.18 | 60 |
| **Surender and Balakumar**[14] | Melamine | Freeze–Drying | 98.8 | 40 |
| **Attri et al.**[15] | Melamine | Thermal Exfoliation | 98.4 | 60 |

a melamine-derived control, surface area and optical characterizations, reactive-species trapping studies, and catalyst-stability studies to evaluate long-term performance under repeated photocatalytic cycles.

## AFFILIATIONS AND AUTHOR DETAILS


### Undergraduate Author

**Hashim Zaki Alsadah** – *Department of Materials Science and Engineering, King Fahd University of Petroleum & Minerals, Dhahran 31261, Saudi Arabia*; 0009-0003-9565-4866
Email: s202335890@kfupm.edu.sa

### Corresponding Author

**Muhammad Ihsan-Ul-Haq** – *Research Mentor, Assistant Professor, Department of Materials Science and Engineering, King Fahd University of Petroleum & Minerals, Dhahran 31261, Saudi Arabia*; 0000-0001-9288-0890
Email: muhammad.ihsanulhaq@kfupm.edu.sa


## ACKNOWLEDGMENTS

The authors are grateful to the staff at the Core Research Facilities of KFUPM for their assistance in acquiring the SEM and TEM images. M. I.-U.-H. acknowledges the Interdisciplinary Research Center for Sustainable Energy Systems for support received under grant no. INSE 2517.

## REFERENCES


(1) Wang, X. *et al.* A metal-free polymeric photocatalyst for hydrogen production from water under visible light. *Nat. Mater.* **8**, 76–80 (2009).

(2) Bhanderi, D., Lakhani, P. & Modi, C. K. Graphitic carbon nitride (g-C3N4) as an emerging photocatalyst for sustainable environmental applications: a comprehensive review. *RSC Sustain.* **2**, 265–287 (2024).

(3) Zhang, Q., Liu, X., Chaker, M. & Ma, D. Advancing Graphitic Carbon Nitride-Based Photocatalysts toward Broadband Solar Energy Harvesting. *ACS Mater. Lett.* **3**, 663–697 (2021).

(4) Timoner, R. L. *et al.* Use of graphitic carbon nitrides as solar-light-driven photocatalysts for the reduction of p-nitrobenzoic acid. *Catal. Today* **434**, 114674 (2024).

(5) Li, C., Harikrishnan, L., Ding, L., Pitcheri, R. & Qi, K. Graphitic carbon nitride-based photocatalysts and sonocatalysts for energy and environment. *Renew. Sustain. Energy Rev.* **226**, 116435 (2026).

(6) Farooq, N. *et al.* Recent advances, synthetic and adaptive approaches of graphitic carbon nitride based nanocomposites towards sustainable applications: A review. *Int. J. Hydrog. Energy* **180**, 151763 (2025).

(7) Abass, G. F., Ahmad, A., Yang, C., Liu, Y. & Frankcombe, T. J. Reassessing structural models of graphitic carbon nitride for reliable photocatalytic predictions. *Mater. Adv.* **7**, 4234–4247 (2026).

(8) Li, Y. *et al.* Construction of a graphitic carbon nitride-based photocatalyst with a strong built-in electric field via $\pi-\pi$ stacking interactions boosting photocatalytic CO 2 reduction. *J. Mater. Chem. A* **12**, 7807–7816 (2024).

(9) Wang, Y.-D., Lee, T.-W., Lo, Y.-C., Hong, W.-J. & Chen, C. Insights into photochemical stability of graphitic carbon nitride-based photocatalysts in water treatment. *Carbon* **175**, 223–232 (2021).

(10) Paušová, Š. *et al.* Photochemical stability of g-C3N4 in the gas phase. *J. Environ. Chem. Eng.* **10**, 107647 (2022).

(11) A, R. *et al.* A Review of Graphitic Carbon Nitride in Photocatalysts: Mechanisms, Synthesis, and Modification. *Top. Curr. Chem.* **384**, 7 (2026).

(12) Torres-Pinto, A., Silva, C. G., Faria, J. L. & Silva, A. M. T. The effect of precursor selection on the microwave-assisted synthesis of graphitic carbon nitride. *Catal. Today* **424**, 113868 (2023).

(13) Ganesan, S., Kokulnathan, T., Sumathi, S. & Palaniappan, A. Efficient photocatalytic degradation of textile dye pollutants using thermally exfoliated graphitic carbon nitride (TE–g–C3N4). *Sci. Rep.* **14**, 2284 (2024).

(14) Surender, S. & Balakumar, S. Insight into the melamine-derived freeze-dried nanostructured g-C3N4 for expeditious photocatalytic degradation of dye pollutants. *Diam. Relat. Mater.* **128**, 109269 (2022).

(15) Attri, P. *et al.* Precursor-dependent fabrication of exfoliated graphitic carbon nitride (gCN) for enhanced photocatalytic and antimicrobial activity under visible light irradiation. *J. Clean. Prod.* **422**, 138538 (2023).

(16) Landge, A. *et al.* Structural, optical, and photocatalytic properties of graphitic carbon nitride. *Mater. Sci. Eng. B* **324**, 119066 (2026).

(17) Chand, H., Kumar, A., Goswami, S. & Krishnan, V. Comparison of catalytic activity of graphitic carbon nitrides derived from different precursors for carbon dioxide conversion. *Fuel* **357**, 129757 (2024).

(18) Shao, Y. *et al.* Piezocatalytic performance difference of graphitic carbon nitride (g-C3N4) derived from different precursors. *Chem. Phys. Lett.* **801**, 139748 (2022).

(19) Tong, Y. *et al.* Recent advances in the design and preparation of graphitic carbon nitride for photocatalysis. *Chem. Commun.* **61**, 1509–1532 (2025).

(20) Oladoye, P. O., Ajiboye, T. O., Omotola, E. O. & Oyewola, O. J. Methylene blue dye: Toxicity and potential elimination technology from wastewater. *Results Eng.* **16**, 100678 (2022).

(21) Khan, I. *et al.* Review on Methylene Blue: Its Properties, Uses, Toxicity and Photodegradation. *Water* **14**, 242 (2022).

(22) Li, S., Cui, Y., Wen, M. & Ji, G. Toxic Effects of Methylene Blue on the Growth, Reproduction and Physiology of Daphnia magna. *Toxics* **11**, 594 (2023).

(23) Molaei, P. & Rahimi-Moghadam, F. Porous g-C3N4 nanosheets through facile thermal polymerization of melamine in the air for photocatalyst application. *J. Mater. Sci. Mater. Electron.* **32**, 19655–19666 (2021).